2025-01-8591 Published 01 Apr 2025

Comprehensive Techno-Economic Analysis of Battery-Electric Trucks: Evaluating Battery Aging Impact for Regional Delivery Missions

Trentalessandro Costantino, Matteo Acquarone, Federico Miretti, and Ezio Spessa Politecnico di Torino

Citation: Costantino, T., Acquarone, M., Miretti, F., and Spessa, E., "Comprehensive Techno-Economic Analysis of Battery-Electric Trucks: Evaluating Battery Aging Impact for Regional Delivery Missions," SAE Technical Paper 2025-01-8591, 2025, doi:10.4271/2025-01-8591.

Received: 30 Oct 2024 Revised: 18 Dec 2024 Accepted: 21 Jan 2025

Abstract

This study presents a detailed techno-economic assessment of battery-electric trucks, incorporating battery aging effects within a total cost of ownership (TCO) model. With increasingly stringent emissions regulations, battery-electric trucks are becoming a viable solution in Europe. However, due to uncertainty regarding their long-term cost-effectiveness and fleet operators' profit-oriented priorities, there is an urgent need for accurate TCO assessment. Existing studies often overlook or oversimplify the impact of battery aging on overall costs. This work addresses this gap by introducing battery aging-related costs through an empirical battery degradation model, evaluated over the vehicle's lifetime. Key aging costs include a refined estimation of battery residual value, influenced by degradation and remaining battery life, and potential battery replacement expenses. A case study on a VECTO group 9 truck used for regional delivery missions examines different payloads and battery pack sizes. Furthermore, we consider two different end-of-life (EoL) threshold scenarios for the battery pack, which impact battery replacement expenses and the truck's residual value. Costs are categorized as battery-independent or battery-dependent, with battery-dependent costs covering purchase price, energy carrier, residual value, and battery replacement cost. In addition to battery aging that impacts both replacement costs and residual value, the results indicate that energy carrier cost is among the most significant economic factors.

Keywords

Total cost of ownership, electric vehicle, battery aging, battery sizing

Introduction

In 2024, the European Council approved a regulation aimed at strengthening the EU CO2 emission standards for heavy-duty vehicles [1]. This regulation seeks to reduce emissions and promote the adoption of zero-emission vehicles, including Battery Electric Vehicles (BEVs) and Fuel Cell Electric Vehicles (FCEVs). The updated targets call for a 45% reduction in emissions by 2030, a 65% reduction by 2035, and a 90% reduction by 2040 for medium lorries, heavy trucks over 7.5 tonnes, and coaches.

Zero-emission vehicles are defined as those that either lack an internal combustion engine or emit no more than 1 gCO2 per kilometer. Consequently, the market share of BEVs, FCEVs, and hydrogen internal combustion engine vehicles (H2-ICEVs) is expected to increase. hence, the main focus of this study is one of these green solutions, i.e., the BEV trucks.

A significant challenge to the growth of BEV truck market share, alongside with the range anxiety and the lack of well established recharging infrastructure, is battery aging and the associated replacement costs throughout the vehicle's lifecycle. Battery degradation poses a critical concern for fleet operators, prompting numerous studies to investigate its processes [2, 3]. Despite this focus, there is a notable gap in research regarding the impact of battery degradation on the lifecycle of heavy-duty vehicles. Existing models frequently overlook empirical data on battery capacity loss, instead relying on simplistic replacement schedules [4, 5, 6, 7, 8, 9]. Additionally, previous studies on battery aging in hybrid electric vehicles [10] have not incorporated robust empirical models to accurately represent these aging phenomena.

Furthermore, there is no consensus on the end-of-life (EoL) criteria for batteries used in transportation applications. Many studies consider the EoL to be reached when the state of health of the battery pack falls to 80% [11, 12], while others propose a lower threshold of 70% [13, 14].

© 2025 The Authors; Published by SAE International. This Open Access article is published under the terms of the Creative Commons Attribution License (http://creativecommons.org/licenses/by/4.0/), which permits distribution, and reproduction in any medium, provided that the original author(s) and the source are credited.

This study aims to enhance the total cost of ownership (TCO) for heavy-duty BEVs by quantifying costs associated with battery capacity loss. By integrating an empirical battery degradation model into the techno-economic analysis, we improve the assessment of the battery's residual value, which is directly linked to the expected mileage before the battery reaches its EoL. Additionally, we account for battery replacement costs. We analyze two different EoL thresholds (80% and 70%) to examine the economic implications for fleet operators, particularly given the absence of regulations regarding minimum performance requirements in term of duration for heavy-duty vehicle battery packs.

Our methodology involves developing a simulation model that accurately represents vehicle characteristics and battery aging. Additionally, we perform a comprehensive economic evaluation using an innovative TCO model. This model assesses various truck configurations with different battery packs and includes costs associated with battery replacement, enhanced residual value, considering two distinct EoL threshold scenarios.

Methods

Simulation Model

The heavy-duty truck model, which incorporates powertrain dynamics and battery aging, is used to simulate real-world vehicle usage and quantify the metrics needed for the techno-economic analysis. While the powertrain model is used to obtain the power requested by the battery and the SOC dynamics, the empirical aging model quantifies the battery degradation over its lifetime.

The simulation employs a distance-based backward-facing model with a tactical driver model for proactive braking and SOC simulation. It supports EC-developed distance-based drive cycles, aligning with EU CO2 regulations and future BEV certification standards [15]. JRC tests [16] confirm its real-world accuracy, with fuel consumption variations within ±3.5%. The Regional Distribution cycle was selected for its alignment with the study's objectives.

Simulation Workflow The battery usage is simulated through the simulation workflow, shown in Fig.1, which is designed to mimic the real-world usage of heavy-duty vehicles, with necessary driver stops and charging intervals.

Before starting the simulation, a representative driving scenario, in our case the Regional Delivery (RD), is selected. Based on this driving cycle, we set the required distance $d_{d,\text{due}}$ the vehicle must cover in a day, which we assumed is 300 km for the RD scenario. This assumption aligns with the ambitious goals of the EU EMPOWER project, which sets a target of a reliable range of 300 km for a regional truck in European applications [17]. The simulation can now start, alternating driving and charging modes as follows. On each day, the driving cycle is repeated multiple times until the number of consecutive driving hours h_c exceeds the 4.5 hours limit [18], the battery SOC reaches the lower threshold (set at 20%), or the total distance driven surpasses $d_{d,\text{due}}$. If one of these conditions is met, the vehicle is stopped and the battery is charged: in particular, if h_c is higher than 4.5 hours, the

FIGURE 1 Flow chart of the powertrain simulation and aging profiles.

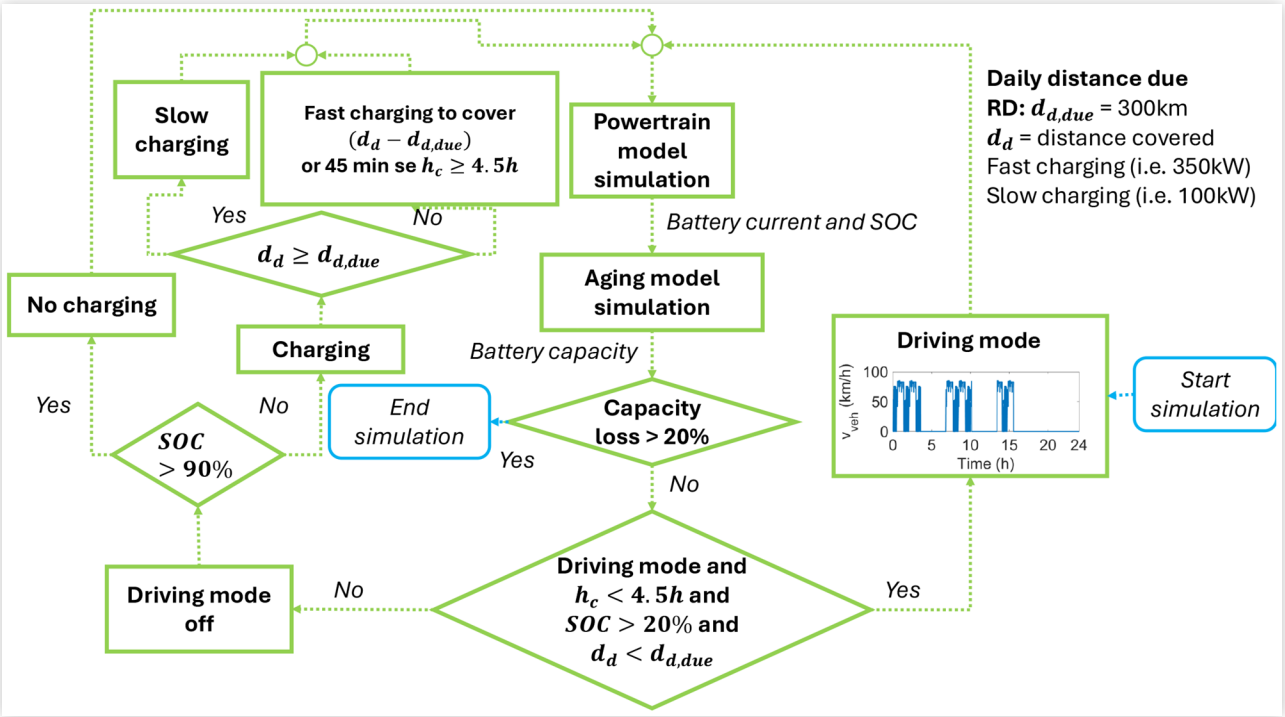

© The Authors

driver must stop for 45 minutes. If the vehicle has not yet covered the daily target distance $d_{d,\text{due}}$, we assume that the driver needs to charge the battery at public fast charging stations, with a power output of 350 kW. Otherwise, if the distance $d_{d,\text{due}}$ is covered, we assume that the truck has reached the fleet operator's depot and can be charged overnight, using slow charging at the lower charging power of 100 kW. The charging phase is stopped when either the maximum SOC (set to 90%) is reached or when the battery has been charged enough to complete the target driving distance $d_{d,\text{due}}$ without requiring additional charging. Once the SOC reaches 90% at the fleet operator's depot, the vehicle remains stationary for the duration of the stop without undergoing any further charging. Finally, when the stop period ends or the next day begins, the whole procedure is repeated. The simulation concludes when the battery reaches its end of life, which in automotive applications is typically defined by an SOH between 70 and 80%. Hence, in this study, we consider two scenarios, with the end of life identified at 70% and 80% SOH, respectively.

Through the described simulation model, we derive different data that will be used in the TCO computation, e.g., the vehicle energy consumption, the distance traveled before the battery reaches its EoL, and the energy required from fast and slow charging stations. In particular, we refer to the energy charged with fast charging and slow charging with the symbols $E_{b,\text{fast}}$ and $E_{b,\text{slow}}$, respectively.

Powertrain Model Relying on the previous works [19, 20], the powertrain is modeled using a backward model approach. In contrast to other backward models, our framework incorporates a behavioral driver model and can accommodate distance-based drive cycles, where the vehicle speed and the road gradient are expressed as a function of traveled distance.

First, the required tractive force F_{veh} is obtained through the longitudinal dynamics equations, accounting for the grade F_{grade}, aereodynamic F_{aero}, rolling F_{roll} resistances and inertia $m_{veh}a_{veh}$:

$$F_{\text{veh}} = F_{\text{roll}} + F_{\text{grade}} + F_{\text{aero}} + m_{veh}a_{veh}, \tag{1}$$

$$F_{\text{roll}} = C_r m_{\text{veh}} g \cos\left(s_{\text{road}}\right), \tag{2}$$

$$F_{\text{grade}} = m_{\text{veh}} g \sin\left(s_{\text{road}}\right), \tag{3}$$

$$F_{\text{aero}} = \frac{1}{2}\rho_{\text{air}} C_d A\left(v_{\text{veh}}\right) v_{\text{veh}}^2. \tag{4}$$

where C_r is the rolling coefficient, m_{veh} is the vehicle mass, v_{veh} is the vehicle speed, s_{road} is the road slope, and ρ_{air} is the air density. Then, the electric motor speed ω_{em} and torque T_{em} and electric power are computed as follows:

$$\omega_{\text{em}} = \frac{v_{\text{veh}}}{r_{\text{wh}}}\tau_{\text{fd}}\tau_{\text{gb}}, \tag{5}$$

$$T_{\text{em}} = \frac{F_{\text{veh}} r_{\text{wh}}}{\tau_{\text{fd}}\tau_{\text{gb}}}, \tag{6}$$

$$P_{\text{b}} = P_{\text{em,el}} = \left(\eta_{\text{em}}\left(\omega_{\text{em}}, T_{\text{em}}\right)\right)^k \omega_{\text{em}} T_{\text{em}}. \tag{7}$$

where r_{wh} is the wheel radius, τ_{gb} and τ_{fd} are the gearbox and final drive ratios, respectively, η_{em} is the motor efficiency, mapped as a function of ω_{em} and T_{em}, and k is a factor equal to -1 and 1 in motor and generator modes, respectively. Finally, the power required to the battery pack P_{b} is equal to the power drawn by the electric motor.

The battery pack is modeled from the electrical standpoint to quantify the battery current (necessary to compute capacity degradation) and SOC dynamics. Each battery cell is modeled as a zero-order equivalent circuit model (ECM), characterized by the ECM parameters internal resistance $R_{0,cell}$ and open circuit voltage OCV_{cell} [21]. Since the battery aging model used in this work is for single battery cells, the pack-level battery power P_{b} is downscaled to the cell-level P_{cell} using the number N_S series-connected and N_P parallel-connected cells of the pack, and the battery SOC is computed through Coulomb counting:

$$P_{cell}\left(t\right) = \frac{P_b\left(t\right)}{N_P N_S} \tag{8}$$

$$I_{cell}\left(t\right) = \frac{OCV_{cell} - \sqrt{OCV_{cell}^2 - 4R_{0,cell}P_{cell}}}{2R_{0,cell}} \tag{9}$$

$$SOC\left(t\right) = SOC\left(t_0\right) + \frac{\int_{t_0}^{t} I_{cell}\left(t\right)dt}{Q_{cell}\left(t\right)} \tag{10}$$

where t_0 is the initial time of the simulation, I_{cell} is the cell current, and Q_{cell} is the actually available cell capacity.

Battery Aging Model During the vehicle's lifetime, EV batteries undergo a progressive degradation process. Neglecting the internal resistance increase [22], in this work, we modeled only the capacity fade [23]. The capacity loss model accounts for calendar aging $Q_{loss,cal}$ and cycling aging $Q_{loss,cyc}$. While calendar aging accounts for those degradation phenomena that occur while the cell is not in use, cycling aging occurs when the battery is subject to driving or charging loads.

Calendar aging is modeled as a function of time and storage conditions, identified by battery temperature and SOC [24]. To use the model in dynamic conditions where the SOC and temperature change over time, such as

real-world EV scenarios, the capacity fade dynamics due to calendar aging are differentiated as in [23]:

$$\frac{dQ_{loss,cal}}{dt} = z_{cal}\left(SOC\right)B_{cal}\left(SOC\right)e^{-\frac{Ea_{cal}}{RT}}t^{z_{cal}\left(SOC\right)-1} \quad (11)$$

where B_{cal} is a factor depending on SOC, Ea_{cal} is the activation energy for calendar aging, T is the battery temperature, and z_{cal} is a dimensionless constant. All these parameters' values are taken from [23].

On the other hand, cycling aging is expressed as a function of operating conditions, i.e., temperature, and charge and discharge C-rate. It is worth noting that in our study, the battery temperature is assumed to be constant due to the assumption of a moderate ambient temperature, which allows the thermal management system to maintain a stable battery pack temperature. Relying on the model proposed in [25], the capacity loss variation due to cycling $\frac{dQ_{loss,cyc}}{dt}$ is written as follows:

$$\frac{dQ_{loss,cyc}}{dt} = \frac{|I|}{3600}z_{cyc}B_{cyc}\left(C\right)e^{-\frac{Ea_{cyc}+\alpha C}{RT}}Ah_{cell}^{z_{cyc}-1}; \quad (12)$$

where B_{cyc} is a factor function of C-rate C, Ea_{cyc} is the activation energy for cycling aging, and z_{cyc} is a dimensionless constant. All these parameters' values are borrowed from [25].

Finally, the total cell degradation Q_{loss} is obtained as a combination of calendar and cycling effects through the following equations:

$$\frac{dQ_{loss}}{dt} = \frac{dQ_{loss,cal}}{dt} + \frac{dQ_{loss,cyc}}{dt} \quad (13)$$

$$Q_{loss} = \int_{t_0}^{t_f}\frac{dQ_{loss}}{d\tau}d\tau \quad (14)$$

TCO

The TCO provides a holistic view of the financial implications of owning and operating an asset over its entire lifespan [26], considering not only the acquisition cost but also ongoing maintenance, operation, and potential expenses [27, 28].

TCO costs are categorized in different ways. First, they can be divided into purchase, operating, and residual value costs. For trucks, the purchase cost is the initial expense for acquiring the vehicle. Operating costs, which form a significant part of TCO, cover energy consumption (fuel or electricity), maintenance, repairs, and consumables (e.g., urea, lubricants). The residual value is the asset's worth at the end of its lifespan, defined as 700,000km in line with the Euro 7 draft [29].

Secondly, a distinction is made for BEV trucks between battery-dependent and battery-independent costs. Battery-dependent costs vary with battery size, while battery-independent costs do not. This study focuses on analyzing battery-dependent costs in particular.

The TCO model was refined from a previous study [20] to assess the fixed and variable costs of BEV vehicles over their entire life cycle from a fleet operator's perspective. Specifically, compared to the prior study, we improved the estimation of the residual value, the energy carrier cost by incorporating battery aging, and the battery replacement cost. These costs include:

- Purchase cost (battery dependent);
- Ownership and operation taxes, including highway tolls (battery independent);
- Driver cost (battery independent);
- Maintenance and repair costs (battery independent);
- Energy carrier cost (battery dependent);
- Battery replacement cost (battery dependent);
- Residual value (battery dependent).

The primary output is the TCO, calculated as the net present value (NPV) of all incurred costs. NPV accounts for the time value of money, representing the present value of future cash flows (CF) discounted at a rate (r):

$$NPV = \sum_{t=0}^{n}\frac{CF_t}{\left(1+r\right)^t}. \quad (15)$$

A 10% discount rate is applied to evaluate the NPV of operational costs year by year throughout the analysis period. The TCO main assumptions are reported in Table 1. Notably, financing costs were excluded from the analysis, as it was assumed that the fleet operator purchases the truck without relying on financial assistance.

Purchase Cost With no mass production for group 9 VECTO BEVs equipped with a 350 kW e-motor in a 6x2 configuration, actual purchase costs are unavailable. The following estimation method is used:

- Start from the purchase cost of a conventional group 9 VECTO truck.
- Remove subsystems not required for BEVs (e.g., conventional powertrain, driveline, aftertreatment).

TABLE 1 TCO Model Assumptions

Parameters	Assumptions
Analysis period	700000 km driven
Annual mileage	73000 km driven
Discount rate	10%
Inflation	Average inflation over the last twenty years in Europe
Taxes	All taxes linked to the truck ownership and operation
Road tolls	Included
External costs	Excluded
Financial benefits	Excluded

© The Authors

TABLE 2 Battery system parameters

Chemistry	Specific Energy (Wh/kg)	Average Cost (EUR/kWh)	Integration Factor
LFP	103	130	2.5

© The Authors

- Add necessary BEV components (e.g., battery, motor, inverter), applying integration factors to component prices from literature.

The purchase cost of a conventional rigid truck with three axles is estimated at 170,000 EUR in 2022, consistent with other studies [4, 30, 20]. Table 2 shows the key battery system parameters used in this study.

Taxes, Road Tolls, Driver Cost and Maintenance Taxes were averaged across European countries, with ownership (993.5 EURO/year), insurance (3000 EURO/year), and highway tolls (0.152 EURO/km) [4] calculated using the NPV formula, while one-time registration taxes (379 EURO) were excluded [31, 32].

Driver costs, based on Comite National Routier data [32], amount to 48,409 EURO/year or 26.59 EURO/hour, considering 1,847 hours of driving.

Maintenance is reduced by 30% for BEVs compared to diesel trucks [33, 4, 30]. The maintenance cost is battery independent because it is function of the distance driven. In fact, in our model, maintenance data is sourced from [4] and includes repair and preventive maintenance, which costs 8.04 €/km, and tires. Tire costs are further subdivided into those for the front and driven axles (2.47 €/km) and for the trailer tires (2.73 €/km).

Energy Carrier Cost The energy carrier cost includes the expense of recharging the vehicle, considering both energy consumption and associated infrastructure costs. BEVs typically recharge at two types of stations: low-power stations at fleet depots (up to 100 kW) and public fast-charging stations (around 350 kW). Our cost model incorporates both charging scenarios. For a more detailed explanation of the equations and methodology used, please refer to the previously published study [20].

While electricity cost data is sourced from EUROSTAT [34], focusing on non-domestic consumers, infrastructure costs are adjusted for inflation based on [4]. The proportion of energy from public fast chargers is influenced by the truck's range and energy requirements and is calculated from the vehicle simulation. The selected parameters are reported in Table 3. In this study, the utilization ratio (UT) serves as a key metric to evaluate the operational efficiency of recharging infrastructure. As defined in [4], it represents the ratio of the annual energy output sold by the infrastructure owner to the maximum capacity of the infrastructure. Essentially, the UT indicates the number of trucks recharged annually per charger. The selected UT values reflect an average usage scenario, as detailed in [20]. all other parameters of Table 3 in this analysis are derived from the established cost model developed in the previously cited study.

TABLE 3 Recharging infrastructure parameters

Recharging technology	Slow charging station	Fast charging station
Utilization ratio (%)	20	5
Annual weeks	52	52
N° Operation per week	6	6
Charging power (kW)	100	350
Charging efficiency (%)	95	95
Internal rate of return (%)	4	10
Service life (y)	15	10
Tariff (EURO/kWh)	0.30	0.52

© The Authors

Battery Replacement The battery replacement cost is often overlooked in techno-economic analyses. In this study, we assume that fleet operators incur the full cost of a new battery pack without discounts for replacements, as they are also responsible for disposal or second-life applications. Consequently, the residual value of a battery pack when it reaches the EoL (depending on the scenario chosen) is treated as a sunk cost.

Battery replacement occurs when the capacity loss reaches 20% or 30%, quantified by the previously introduced aging model. As previously mentioned, we consider two scenarios for replacement to account for the different possible regulatory scenarios: one replaces the battery at 80% state of health (SOH) while the other at 70% SOH. The total cost is calculated using the NPV formula, taking into account the replacement ratio derived from the truck's lifespan compared to the battery lifespan.

Residual Value Determining a truck's residual value is complex since it is influenced by both age and mileage. Following the methodology outlined by Burnham et al. [35], we use an exponential function to assess the truck's depreciation, quantifying its value without the battery pack.

For complete BEV trucks, we followed the proposed new approach to estimate the battery pack's residual value, which depends on its remaining capacity at the vehicle's end of life [36]. The model first identifies when the last battery replacement occurs, based on the replacement ratio and battery lifespan. It then calculates the remaining distance the truck can travel after this replacement and before reaching the end of its operational life.

Using the simulation model, we estimate the battery's capacity loss over this distance to determine its residual capacity at the vehicle's end of life. A linear interpolation method is then employed to compute the battery pack's residual value.

Finally, we combine the truck's residual value (excluding the battery) with the estimated residual value of the battery to derive the total residual value of the BEV truck.

Results

Simulation Results

This study centers on a techno-economic analysis of a regional delivery VECTO Group 9 truck.

Different payloads and battery pack sizes are simulated and analyzed to provide a thorough analysis of different truck configurations useful for the techno-economic assessment. Here, we evaluate different percentages of the maximum payloads (e.g. 0, 25, 50, 75, 100 percent), and various battery pack sizes (e.g. 282, 376, 470, 564, 658, 752, 846, 940 kWh of nominal energy) through the simulation model detailed in the Methods section. Since we study two EoL scenarios, 90 TCO configurations are assessed.

Simulation Model Results

The main parameters of the group 9 rigid truck are detailed in Table 4. The data, collected in Table 4, pertaining to the truck glider, including parameters such as wheel specifications, rolling resistance coefficient, final drive ratio, and gearbox configuration, are sourced from the VECTO European certification software, prior work [19, 20] (e.g., E-machine characteristics), and informed assumptions (e.g., battery nominal energy).

Following the previously illustrated simulation workflow, we quantify the battery capacity loss profiles until battery EoL for the different battery pack configurations. As previously mentioned, from the simulation model, we obtain the vehicle energy consumption, the distance traveled before the battery reaches its EoL, and the energy required from fast and slow charging stations.

It is worth highlighting that, as the battery ages, the energy charged with fast charging rises in comparison to the energy charged through slow charging, as shown in Figs. 2a and 2b. This phenomenon is due to the battery capacity degradation over its lifetime. Indeed, as the capacity gets lower, the battery is discharged faster, reaching the lower SOC limit sooner. Hence, the vehicle is stopped more often to recharge at public fast charging stations. Fig. 2a presents the energy supplied to the vehicle over its operational life (E_b). This graph proves that, while the slow charging energy is linear with the distance traveled because not highly affected by battery aging, the fast charging energy increases at an accelerating rate over the battery lifetime. Moreover, Fig. 2b helps to highlight that the fraction between the fast charging energy and the total charging energy ($E_{b,\text{fast}} + E_{b,\text{slow}}$) increases from 15% at beginning of life to almost 35% at the end of life. These results show the importance of considering battery aging not only to obtain the battery replacement costs but also to quantify the energy carrier cost that is drastically influenced by the ratio between fast charging

FIGURE 2 Profile for the maximum payload and battery size of 470kWh truck configuration. (a): Fast and slow charging energy. (b): Percentage of fast charging relative to the total charging energy.

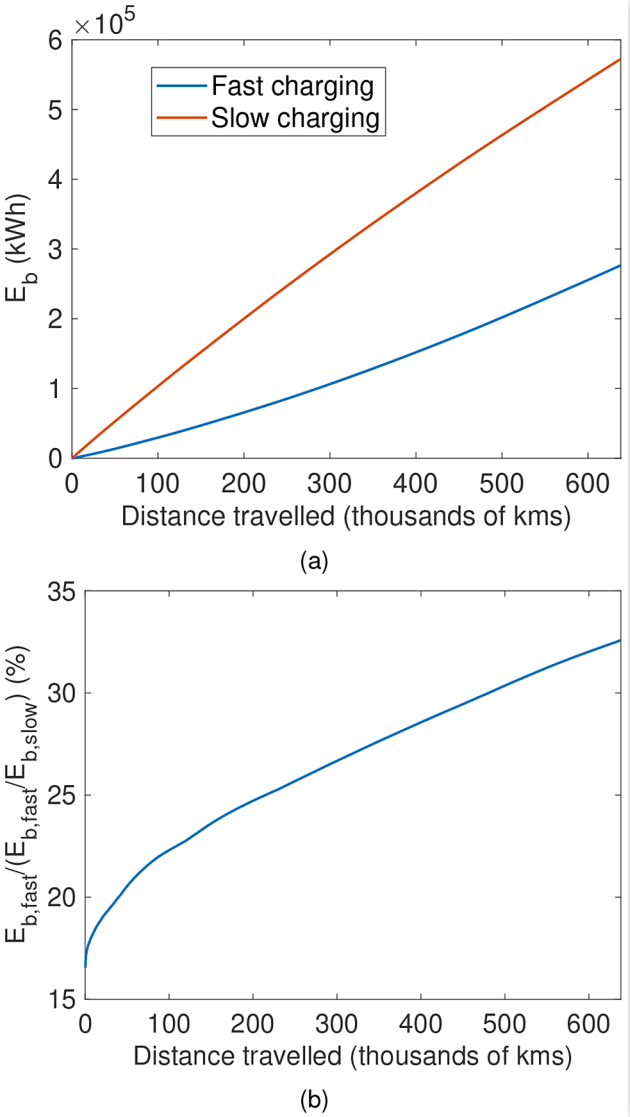

© The Authors

TABLE 4 BEV Main vehicle parameters.

Component	Parameter	Value
Vehicle	Glider mass	11.7 tons
	Gross mass	28 tons
	Wheel radius	0.507 m^2
	Drag area C_dA	5.2 m^2
	Rolling resistance coefficient C_r	0.0057
Final drive	Speed ratio τ_{fd}	2.59
	Efficiency	0.98
Gearbox	Speed ratios τ_{gb}	{3.86, 1.93}
	Efficiency	{0.95, 0.95}
E-machine	Rated Power	350 kW
	Maximum torque	1358 Nm
Battery	Nominal voltage	710 V
	Nominal energy	470kWh
	Chemistry	LFP

© The Authors

and slow charging energies. This increasing ratio also poses a logistical challenge for drivers, who must find public fast-charging stations more frequently throughout the vehicle's ownership period.

TCO Results

In this section, we present the TCO results, analyzing the 9 different battery pack configurations considered with various payloads under two distinct EOL scenarios for truck battery packs. A significant distinction between the two scenarios is the number of battery replacements: replacing the battery at 70% SOH generally leads to much fewer battery pack replacements than 80% SOH, as depicted in Figure 3 and 4. This phenomenon occurs because capacity fading does not follow a linear trend over distance traveled or time elapsed; instead, it exhibits a negatively exponential pattern. Initially, the capacity loss is more pronounced, but as the distance traveled increases, the rate of capacity loss diminishes.

An interesting finding is that, since we assumed a daily mileage of 300 km, very large battery packs do not offer any advantage in reducing energy carrier costs. With smaller battery packs, the fast-charging ratio is already low, which is sufficient to meet the mileage requirement without frequent charging. However, the purchase cost for larger battery packs is significantly higher, resulting in an overall cost increase.

These results underscore the importance of tailoring the truck configuration to the specific mission requirements. Selecting the most suitable configuration is key to achieving cost-effective freight transport with zero-tailpipe-emission trucks.

Another important difference reflected in the results is the residual value of the battery packs. As replacements occur at varying intervals, the last battery pack sold by the fleet operator at the end of its life will possess different residual lifetimes in each scenario, resulting in distinct residual values between the configuration with the same battery pack.

TCO When the Battery EoL Is Set to SOH 80% We analyzed nine different battery pack sizes to understand how the TCO changes under varying load conditions, from empty to fully loaded trucks. As outlined in the

FIGURE 3 Breakdown of the TCO for various use cases with the battery's end-of-life (EoL) set at a State of Health (SOH) of 80%. The figure includes five subplots: the first subplot displays the TCO for different battery sizes when the truck is empty, followed by the TCO when the truck is loaded at 25%, 50%, 75%, and finally, at full capacity.

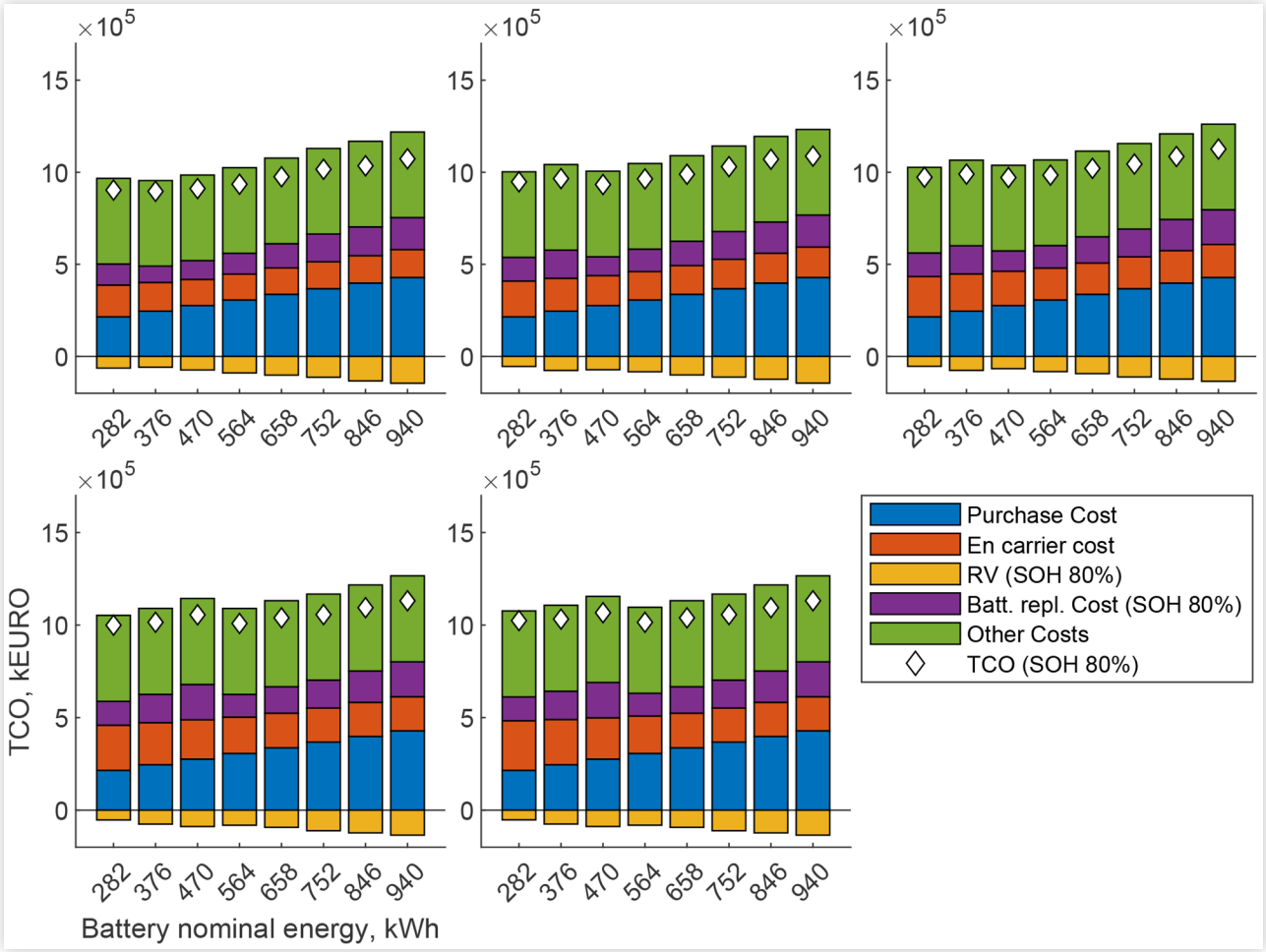

© The Authors

FIGURE 4 Breakdown of the TCO for various use cases with the battery's end-of-life (EoL) set at a State of Health (SOH) of 70%. The figure includes five subplots: the first subplot displays the TCO for different battery sizes when the truck is empty, followed by the TCO when the truck is loaded at 25%, 50%, 75%, and finally, at full capacity.

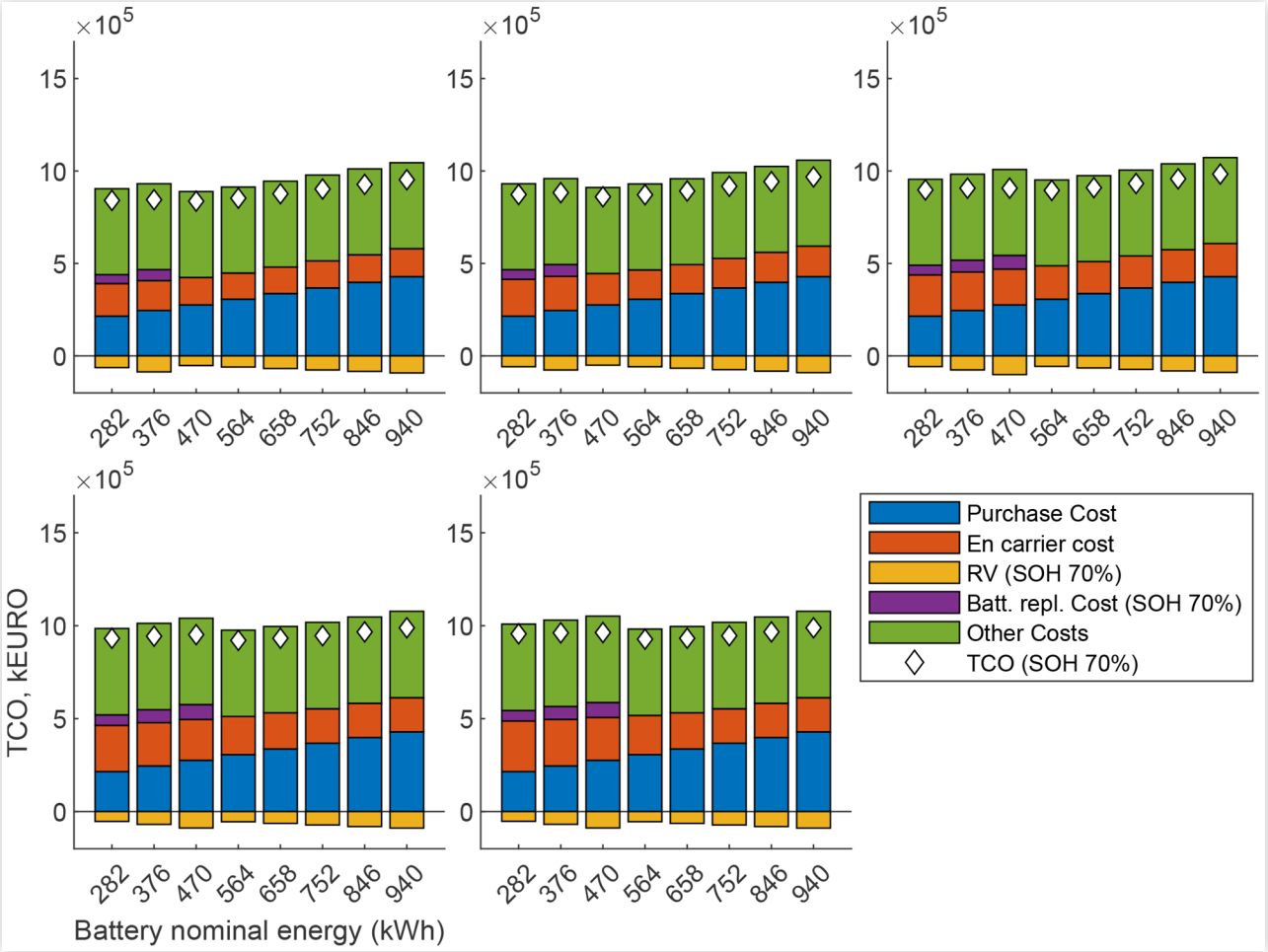

© The Authors

methodology section, we classified the cost components into two categories: battery-dependent and battery-independent costs. In the cost breakdown shown in figure 3, we grouped all battery-independent costs together under "other costs." This category includes expenses such as taxes, highway tolls, maintenance (which is modeled as a function of distance traveled), and driver wages, which remain constant across truck configurations.

Our findings indicate that total truck costs increase with payload. This is primarily due to higher energy consumption under heavier loads, which drives up energy carrier costs and accelerates battery wear. Heavier loads require a greater ampere-hour throughput, impacting battery capacity and longevity. For instance, when comparing an empty truck in the first panel to a truck carrying 75% of its payload in the fourth panel, the 376 kWh and 470 kWh configurations experience an additional battery replacement and a higher energy carrier cost due to the higher load demand. These results highlight the importance of an integrated simulation model that combines economic and technical aspects that, otherwise, might be overlooked.

Generally, the most cost-effective configuration minimizes battery replacements and supports a low fast-charging ratio, thereby reducing energy carrier costs. This dual reduction—fewer battery replacements and lower energy carrier costs—results in the most cost-effective setup across the different payloads. This approach also considers the fleet operator's loss associated with the battery's residual value at EoL. At this point, the residual value of the replaced battery becomes a sunk cost for the fleet operator, as it is transferred to the maintenance center for disposal, dismantling, or potential resale for secondary applications. Although different from zero, any remaining value at EoL is effectively lost from the operator's perspective.

Looking again at the first panel, the most cost-effective option for an empty truck is the 376 kWh battery pack, as it requires only one replacement over the truck's lifespan. As the payload increases, the optimal configuration shifts to larger battery packs, up to 564 kWh for fully loaded scenarios. This shift is due to capacity fade correlated with energy consumption; as payload increases, the energy demand rises accordingly, reducing battery

lifespan. Additionally, larger battery sizes experience reduced cycle aging, further contributing to lower degradation.

Therefore, it is essential to understand each fleet operator's specific business model. If a fleet primarily operates with trucks traveling empty, a smaller battery pack (e.g., 376 kWh) may be optimal. Conversely, if trucks are frequently fully loaded, a larger battery pack would be more suitable.

TCO When the Battery EoL Is Set to SOH 70% As expected, when considering a battery EoL threshold of 70% SOH, there are notably fewer replacements across all battery pack configurations and payload scenarios. Specifically, when the truck operates with zero payload, only the smallest battery packs (282 and 376 kWh) require replacement. For the larger configurations, no replacements are necessary within the truck's operational lifetime. However, as payload increases, even the third-smallest configuration will eventually require a battery replacement.

Overall, the TCO in this scenario is lower compared to the 80% SOH EoL threshold scenario, underscoring the potential benefits of a standardized EoL threshold for batteries especially when we compare different technologies. Despite these differences, the most cost-effective configuration remains consistent, favoring setups that minimize replacements over the truck's lifetime. This configuration has a smaller purchase cost and reduced energy carrier costs, as it relies more on depot charging, avoiding the high costs associated with battery replacements and public fast-charging. This further highlights the importance of developing a cost model closely integrated with technical factors, particularly payload and battery degradation over time, to scientifically compare configurations. This approach ensures a rigorous evaluation that accounts for the real-life performance of each configuration, leading to a more effective and reliable cost analysis.

Another aspect to be considered is the generically lower residual value of the configuration assessed in this EoL scenario compared to the 80% SOH scenario. This is because the remaining life of the battery pack is shorter compared to the other scenario, resulting in a lower residual value. Consequently, the overall residual value, which depends on the battery pack's residual value, is reduced. Note that the residual value of the glider remains unchanged, as both configurations cover the same distance and have the same operational lifespan.

Lastly, in the 70% SOH scenario, energy carrier costs are higher compared to the 80% SOH scenario. This is due to the increased reliance on public fast charging, as noted in Section and illustrated in Figure 2b. The battery fade at 70% SOH drives up the need for fast charging, which is less frequent in the 80% SOH scenario. However, this rise in energy carrier cost remains relatively low, as discussed in, because the overall fast-charging ratio is not high, even with the increase due to battery fade.

Thus, while the additional energy cost impact is almost negligible, this scenario does highlight a technical and logistical challenge. The driver must access more public charging infrastructure, which could pose significant practical limitations.

Conclusion

This study conducted a comprehensive techno-economic analysis of a regional delivery VECTO Group 9 truck, comparing various battery pack sizes and payload scenarios under two battery EoL conditions (i.e. 80% and 70% of the initial SOH). Using simulation modeling, we quantified how battery aging impacts vehicle performance and total cost of ownership (TCO) across different configurations.

Our findings highlight several insights relevant to fleet operators and also for policymakers. First, battery capacity degradation is a critical factor influencing not only the frequency of battery replacements but also the energy carrier cost and the residual value. The impact on the energy carrier cost is driven largely by the increased demand for public fast charging as battery capacity diminishes, as illustrated in Figure 2b, which shows the trend of the fast charging ratio (i.e., the proportion of energy provided by public fast charging stations relative to the total energy required to complete the truck's mission). This ratio increases significantly from the beginning of the battery pack's life to its end of life. For instance, in the illustrated scenario, the fast charging ratio starts at 17% and rises to approximately 32%. This is due to the battery aging phenomena. Given that the cost of energy from public fast charging stations (0.52 C/kWh) is higher than that from private slow charging stations (0.30 C/kWh), as highlighted in Table 3, battery aging has a substantial impact on the annual energy carrier cost. The effect on the truck's residual value is also crucial because in our model we considered the battery residual value directly linked to the residual life of the battery and therefore with the capacity fade. In fact, the aging model enables us to predict the battery's state of health at the end of the truck's lifespan, allowing for a residual value estimation that considers the battery's expected remaining life.

The analysis shows that battery size should be tailored to specific payload requirements and operational patterns. This conclusion is supported by the Results, which show that the truck's TCO minimum for the same daily distance shifts from a nominal battery size of 376 kWh when the truck is empty to 564 kWh when it is fully loaded, in the 80% SOH scenario. For regional distribution missions with set daily mileages, larger battery configurations do not necessarily result in cost savings on energy carriers. This occurs because the fast charging ratio remains essentially unchanged for battery sizes exceeding 658 kWh of nominal energy, when we consider a truck fully loaded, as the ability to complete the chosen daily mission (i.e., 300 km) is already ensured with a battery pack of this size. Instead, if you decide to increase the battery size it will increase overall costs due to the higher purchase cost of the truck driven by the larger battery pack size.

The study further underscores the economic and operational impact of the EoL threshold. An EoL at 70% SOH results in fewer battery replacements over the truck's lifespan compared to an EoL at 80%, reducing TCO by lowering both replacement frequency and associated costs. While the 70% SOH scenario incurs slightly higher energy carrier costs due to increased fast charging needs, the impact remains minimal within the scope of this study's scenarios.

These findings demonstrate the need for a holistic TCO model that integrates both technical and economic factors, including load variability and battery degradation dynamics, to effectively guide fleet operators in selecting cost-effective and sustainable truck configurations tailored to their needs. For policymakers, this study also underscores the importance of standardized battery EoL criteria, especially when comparing BEV with alternative technologies from a techno-economic perspective, as these criteria have a substantial impact on overall results.

Future research should focus on extending this analysis to a broader range of duty cycles, such as longhaul missions and urban missions, and exploring different chemistries or advancements in battery technology that could mitigate fast charging, cycle aging and calendar aging impacts on degradation. Additionally, incorporating real-world data on infrastructure availability and charging patterns will further refine TCO models and support the industry's transition to zero-emission freight transport. Moreover, assessing the impact of thermal management on battery aging and energy carrier costs, as it also affects the truck's available range, will be an important focus. Lastly, conducting a comprehensive Life Cycle Assessment based on the rationale presented here will be essential to understanding the environmental impacts of battery aging over the truck's lifespan, enabling fleet operators and policymakers to make more informed decisions.

Acknowledgement

This project has received funding from the European Union's HORIZON EUROPE research and innovation programme under grant agreement No. 101096028. The content of this publication is the sole responsibility of the Consortium partners listed herein and does not necessarily represent the view of the European Commission or its services.

References

1. "Heavy-Duty Vehicles: Council Signs Off on Stricter CO2 Emission Standards," May 2024.
2. Xiong, R., Li, L., and Tian, J., "Towards a Smarter Battery Management System: A Critical Review on Battery State of Health Monitoring Methods," *Journal of Power Sources* 405 (2018): 18-29.
3. Pinson, M.B. and Bazant, M.Z., "Theory of SEI Formation in Rechargeable Batteries: Capacity Fade, Accelerated Aging and Lifetime Prediction," *Journal of The Electrochemical Society* 160 (2012): A243-A250.
4. Basma, H., "Total Cost of Ownership for Tractor-Trailers in Europe: Battery Electric versus Diesel," tech. Rep., ICCT, 2019.
5. Burke, A., Miller, M., Sinha, A., and Fulton, L., "Evaluation of the Economics of Battery-Electric and Fuel Cell Trucks and Buses: Methods, Issues, and Results," 2022.
6. Noll, B., del Val, S., Schmidt, T.S., and Steffen, B., "Analyzing the Competitiveness of Low-Carbon Drive-Technologies in Road-Freight: A Total Cost of Ownership Analysis in Europe," *Applied Energy* (2022).
7. Alonso-Villar, A., Davidsdottir, B., Stefansson, H., Asgeirsson, E.I. et al., "Technical, Economic, and Environmental Feasibility of Alternative Fuel Heavy-Duty Vehicles in Iceland," *Journal of Cleaner Production* (2022).
8. Sen, B., Ercan, T., and Tatari, O., "Does a Battery-Electric Truck Make a Difference? – Life Cycle Emissions, Costs, and Externality Analysis of Alternative Fuel-Powered Class 8 Heavy-Duty Trucks in the United States," *Journal of Cleaner Production* (2017).
9. Rout, C., Li, H., Dupont, V., and Wadud, Z., "A Comparative Total Cost of Ownership Analysis of Heavy Duty On-Road and Off-Road Vehicles Powered by Hydrogen, Electricity, and Diesel," *Heliyon* (2022).
10. Finesso, R., Spessa, E., and Venditti, M., "An Unsupervised Machine-Learning Technique for the Definition of a Rule-Based Control Strategy in a Complex HEV," *SAE International Journal of Alternative Powertrains* (2016).
11. Nuhic A., Terzimehic T., Soczka-Guth T., Buchholz M., and Dietmayer K., "Health Diagnosis and Remaining Useful Life Prognostics of Lithium-Ion Batteries Using Data-Driven Methods," *Journal of Power Sources*, vol. 239, p. 680 – 688, 2013. Cited by: 553.
12. Lin C.-P., Cabrera J., Yang F., Ling M.-H., Tsui K.-L., and Bae S.-J., "Battery State of Health Modeling and Remaining Useful Life Prediction through Time Series Model," *Applied Energy*, vol. 275, 2020. Cited by: 87.
13. Dong H., Jin X., Lou Y., and Wang C., "Lithium-Ion Battery State of Health Monitoring and Remaining Useful Life Prediction Based on Support Vector Regression-Particle Filter," *Journal of Power Sources*, vol. 271, p. 114 – 123, 2014. Cited by: 268.
14. Catelani, M., Ciani, L., Fantacci, R., Patrizi, G. et al., "Remaining Useful Life Estimation for Prognostics of Lithium-Ion Batteries Based on Recurrent Neural Network," *IEEE Transactions on Instrumentation and Measurement* 70 (2021): 1-11.
15. "Proposal for a Regulation of the European Parliament and of the Council Amending Regulation (EU) 2019/1242 as Regards Strengthening the CO2 Emission Performance Standards For New Heavyduty Vehicles and Integrating Reporting Obligations, and repealing Regulation (EU) 2018/956," vol. COM/2023/88 Final, 2023.

16. Fontaras, G., Grigoratos, T., Savvidis, D., Anagnostopoulos, K. et al., "An Experimental Evaluation of the Methodology Proposed for the Monitoring and Certification of CO2 Emissions from Heavy-Duty Vehicles in Europe," *Energy* (2016).
17. Spessa, E., Accardo, A., Costantino, T., Gentilucci, G. et al., "LCA and TCO Assessment of Baseline Vehicles," Report D1.3, 2024. Grant Agreement No. 101096028, Horizon-CL5-2022-D5-01-08, Type: Innovation Action (IA), Dissemination Level: Public.
18. "Regulation (EC) no 561/2006 of the European Parliament and of the Council of 15 March 2006 on the Harmonisation of Certain Social Legislation Relating to Road Transport and Amending Council Regulations (EEC) no 3821/85 and (EC) no 2135/98 and Repealing Council Regulations (EEC) no 3820/85," *OJ*, vol. L 102, March 2006.
19. Costantino, T., Miretti, F., and Spessa, E., "Improving the Feasibility of Electrified Heavy-Duty Truck Fleets with Dynamic Wireless Power Transfer," 2023.
20. Costantino, T., Miretti, F., and Spessa, E., "Assessing the Viability of Dynamic Wireless Power Transfer in Long-Haul Freight Transport: A Techno-Economic Analysis from Fleet Operators' Standpoint," *Applied Energy* 379 (2025): 124839.
21. Tran, M.-K., DaCosta, A., Mevawalla, A., Panchal, S. et al., "Comparative Study of Equivalent Circuit Models Performance in Four Common Lithium-Ion Batteries: LFP, NMC, LMO, NCA," *Batteries* 7 (2021): 51.
22. Cordoba-Arenas, A., Onori, S., Guezennec, Y., and Rizzoni, G., "Capacity and Power Fade Cycle-Life Model for Plug-In Hybrid Electric Vehicle Lithium-Ion Battery Cells Containing Blended Spinel and Layeredoxide Positive Electrodes," *Journal of Power Sources* 278 (2015): 473-483.
23. Petit, M., Prada, E., and Sauvant-Moynot, V., "Development of an Empirical Aging Model for Li-Ion Batteries and Application to Assess the Impact of Vehicle-to-Grid Strategies on Battery Lifetime," *Applied Energy* 172 (2016): 398-407.
24. Keil, P., Schuster, S.F., Wilhelm, J., Travi, J. et al., "Calendar Aging of Lithiumion Batteries: I. Impact of the Graphite Anode on Capacity Fade," *Journal of The Electrochemical Society* 163, no. 9 (2016): A1872-A1880.
25. Wang, J., Liu, P., Hicks-Garner, J., Sherman, E. et al., "Cycle-Life Model for Graphitelifepo4 Cells," *Journal of Power Sources* 196 (2011): 3942-3948.
26. Ellram, L., "Total Cost of Ownership: An Analysis Approach for Purchasing," *International Journal of Physical Distribution and Logistics Management* 25 (1995): 4-23.
27. Ellram, L.M., "Total Cost of Ownership," in *Handbuch Industrielles Beschaffungsmanagement: Internationale Konzepte — Innovative Instrumente — Aktuelle Praxisbeispiele* (Hahn D. and Kaufmann L., eds.), pp. 659-671, Wiesbaden: Gabler Verlag, 2002.
28. Parkhi S., *Total Cost of Ownership (TCO)*. 2014.
29. "Proposal for a Regulation of the European Parliament and of the Council on Type-Approval of Motor Vehicles and Engines and of Systems, Components and Separate Technical Units Intended for Such Vehicles, with Respect to Their Emissions and Battery Durability (Euro 7) and Repealing Regulations (EC) no 715/2007 and (EC) no 595/2009," vol. COM/2022/586 Final, 2022.
30. Kuhn, "E-Truck Virtual Teardown Study," June 2021.
31. Persyn, D., Diaz-Lanchas, J., and Barbero, J., "Estimating Road Transport Costs between EU Regions," Tech. Rep. 04/2019, Joint Research Group, 2019.
32. "Enquete Longue Distance," tech. rep., Comite National Routier, 2022.
33. Kleiner F. and Friedrich H., "Maintenance and Repair Cost Calculation and Assessment of Resale Value for Different Alternative Commercial Vehicle Powertrain Technologies," 2017.
34. Eurostat, "Electricity Prices for Non-Household Consumers - Bi-Annual Data (from 2007 Onwards)," 2024.
35. Burnham, A., Gohlke, D., Rush, L., Stephens, T. et al., "Comprehensive Total Cost of Ownership Quantification for Vehicles with Different Size Classes and Powertrains," Tech. Rep. ANL/ESD-21/4, Argonne National Lab. (ANL), Argonne, IL, 2021.
36. Costantino, T., Acquarone, M., Miretti, F., and Spessa, E., "Incorporating Battery Aging Phenomena for Cost-Effective Battery Electric Truck Fleets," Submitted to Applied Energy, 2025.

© 2025 The Authors; Published by SAE International. This Open Access article is published under the terms of the Creative Commons Attribution License (http://creativecommons.org/licenses/by/4.0/), which permits distribution, and reproduction in any medium, provided that the original author(s) and the source are credited.

Positions and opinions advanced in this work are those of the author(s) and not necessarily those of SAE International. Responsibility for the content of the work lies solely with the author(s).

ISSN 0148-7191